Photophysics and Reverse Saturable Absorption of Cationic Dinuclear Iridium(III) Complexes Bearing Fluorenyl-Tethered 2-(Quinolin-2-yl)quinoxaline Ligand

Cuifen Lu,[a,b,‡] Taotao Lu,[a,‡] Peng Cui,[c,a,d] Svetlana Kilina,[a] Wenfang Sun[a,*]

[a]Department of Chemistry and Biochemistry, North Dakota State University, Fargo, ND 58108-6050, USA

[b]Hubei Collaborative Innovation Center for Advanced Organochemical Materials & Ministry-of-Education Key Laboratory for the Synthesis and Application of Organic Functional Molecules, Hubei University, Wuhan, 430062, P.R. China

[c]Key Laboratory of Eco-textiles, Ministry of Education, Jiangnan University, Wuxi, Jiangsu Province 214122, P. R. China

[d]Materials and Nanotechnology Program, North Dakota State University, Fargo, ND 58108-6050, USA

‡ These two authors contributed equally to this project.

* Corresponding author. E-mail: Wenfang.Sun@ndsu.edu

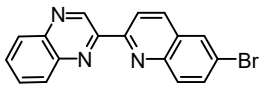
N
N
N
Br

4

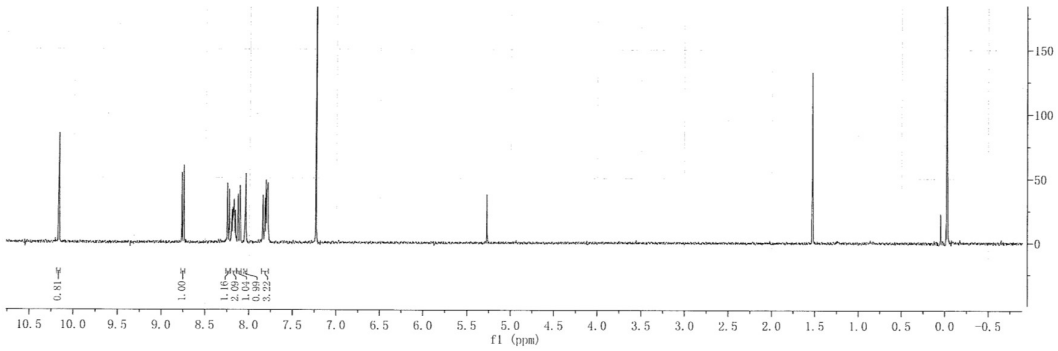
0.81
1.00
1.16
2.09
1.04
3.23
10.5 10.0 9.5 9.0 8.5 8.0 7.5 7.0 6.5 6.0 5.5 5.0 4.5 4.0 3.5 3.0 2.5 2.0 1.5 1.0 0.5 0.0 -0.5
f1 (ppm)
150
100
50
0

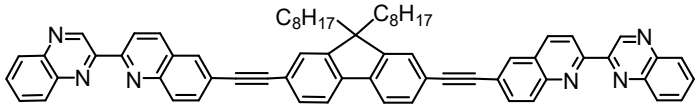
C_8H_{17}
C_8H_{17}
N
N
N
N
N

L-1

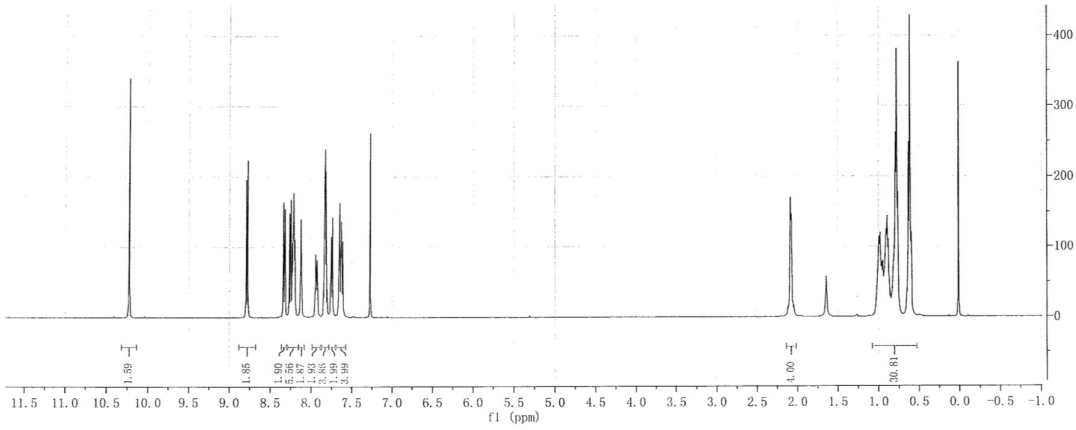
1.59
1.85
1.90
1.86
1.92
3.86
1.99
24.99
4.00
30.81
11.5 11.0 10.5 10.0 9.5 9.0 8.5 8.0 7.5 7.0 6.5 6.0 5.5 5.0 4.5 4.0 3.5 3.0 2.5 2.0 1.5 1.0 0.5 0.0 -0.5 -1.0
f1 (ppm)
400
300
200
100
0

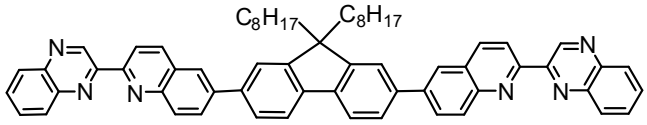
C_8H_{17}
C_8H_{17}
N
N
N
N
N

L-2

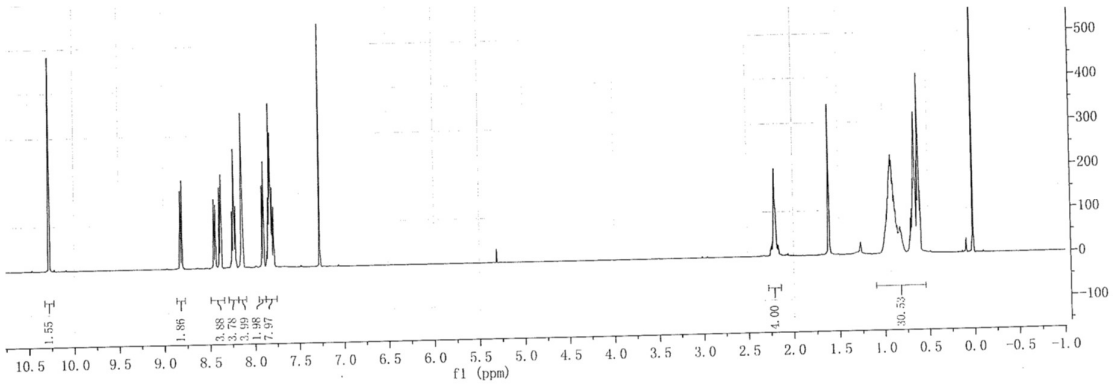
1.55
1.886
3.88
3.78
3.98
1.98
7.97
4.00
30.53
10.5 10.0 9.5 9.0 8.5 8.0 7.5 7.0 6.5 6.0 5.5 5.0 4.5 4.0 3.5 3.0 2.5 2.0 1.5 1.0 0.5 0.0 -0.5 -1.0
f1 (ppm)
500
400
300
200
100
0
-100

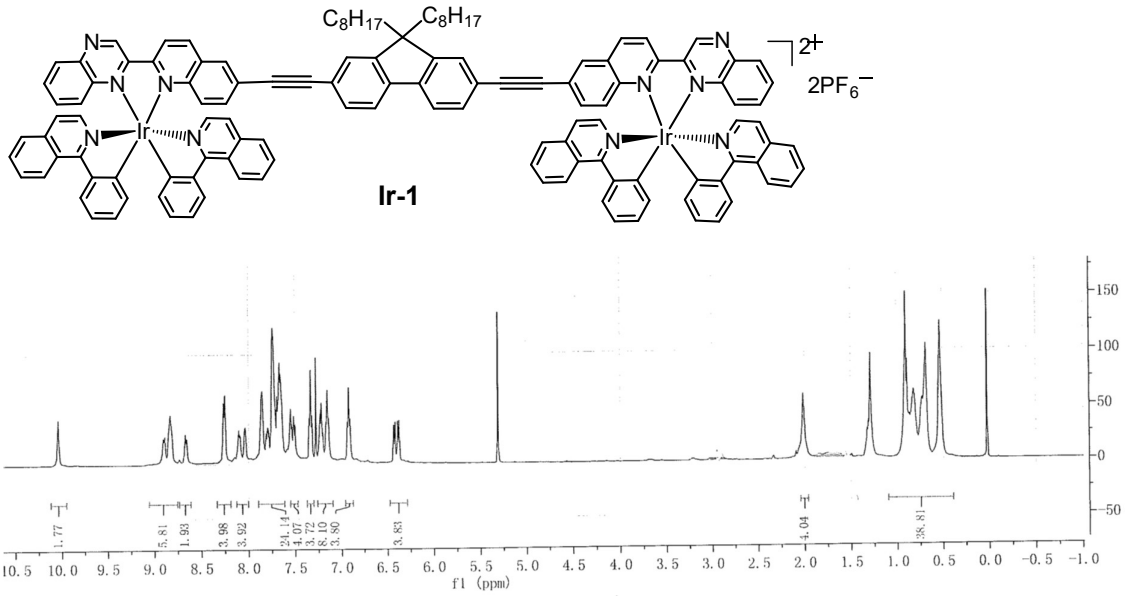

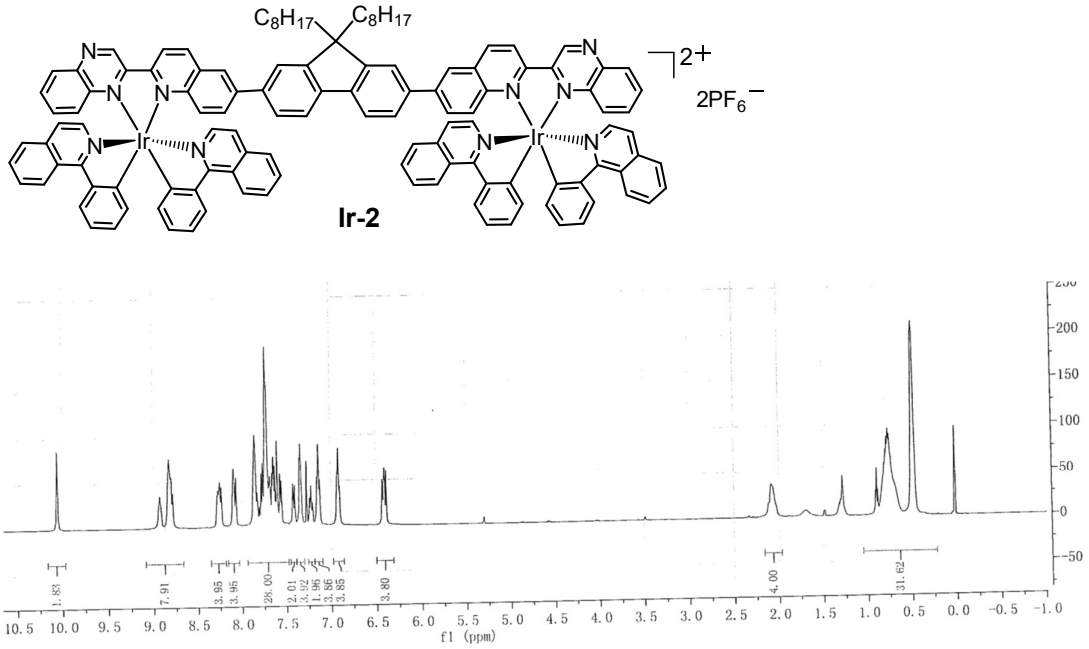

Figure S1. ^{1}H-NMR spectra of compound **4**, ligands **L-1** and **L-2,** and Ir(III) complexes **Ir-1** and **Ir-2** in $CDCl_3$.

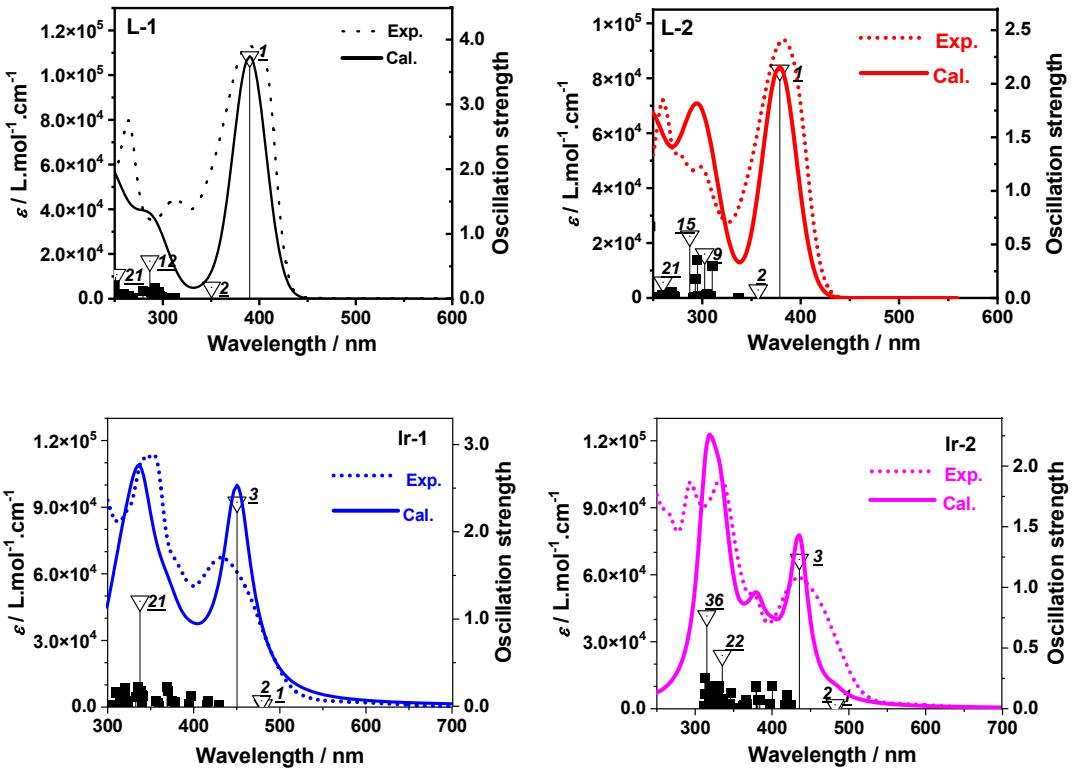

Figure S2. Comparison of the experimental and calculated absorption spectra for **L-1** and **L-2** in CH_2Cl_2, and **Ir-1** and **Ir-2** in CH_3CN. Calculations were performed with linear response TDDFT with PBE1 functional and LANL2DZ/6-31G* basis sets. Vertical line indicates the oscillation strength of the first 70 transitions.

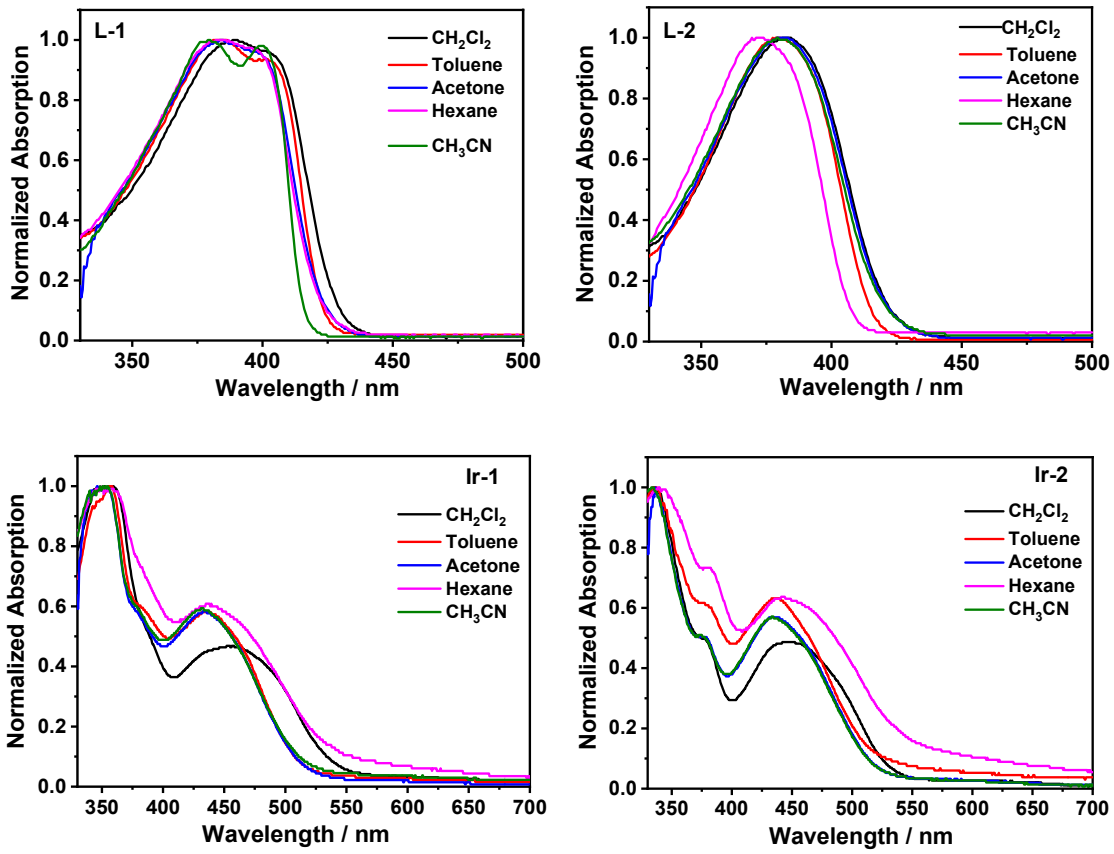

Figure S3. Normalized UV-vis absorption spectra of **L-1**, **L-2**, **Ir-1**, and **Ir-2** in different solvents.

Table S1. Natural transition orbitals (NTOs) representing the main transitions contributing to the high-energy absorption bands for **L-1** and **L-2** in CH_2Cl_2 and **Ir-1** and **Ir-2** in CH_3CN.

	States	Hole	Electron
L-1	S_{12} 286 nm *f*=0.58	 53%  35%	 53% 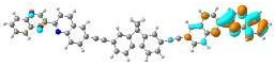 35%
	S_{21} 252 nm *f*=0.37	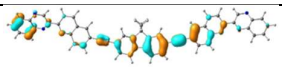 56% 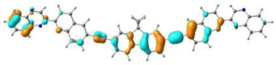 15%	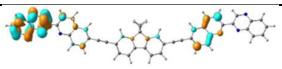 56% 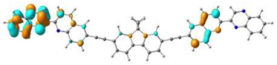 15%
L-2	S_9 303 nm *f*=0.41	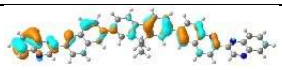 48%  41%	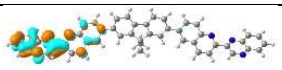 48%  41%
	S_{15} 288 nm *f*=0.58	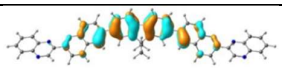 58% 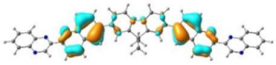 22% 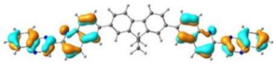 12%	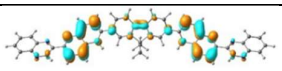 58% 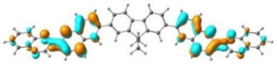 22% 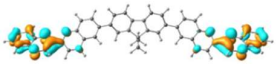 12%
	S_{21} 261 nm *f*=0.15	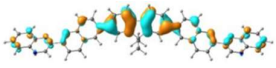 43% 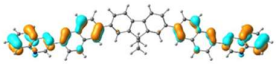 29%	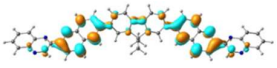 43% 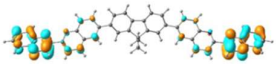 29%
Ir-1	S_{21} 338 nm *f*=1.20	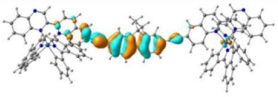 68% 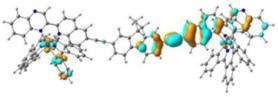 25%	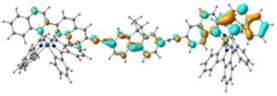 68% 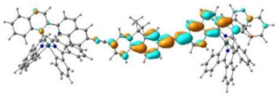 25%
Ir-2	S_{22} 336 nm *f*=0.43	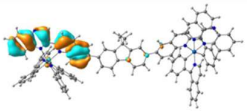 70% 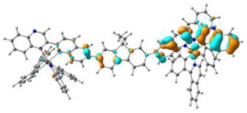 11%	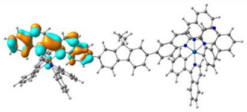 70% 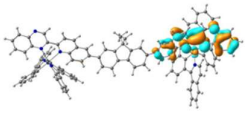 11%

S_{36} 316 nm *f*=0.74	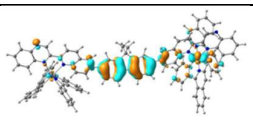 52%	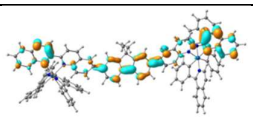 52%
	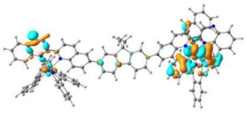 21%	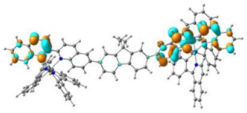 21%
	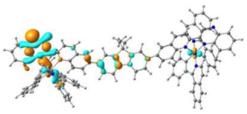 12%	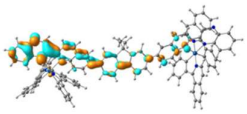 12%

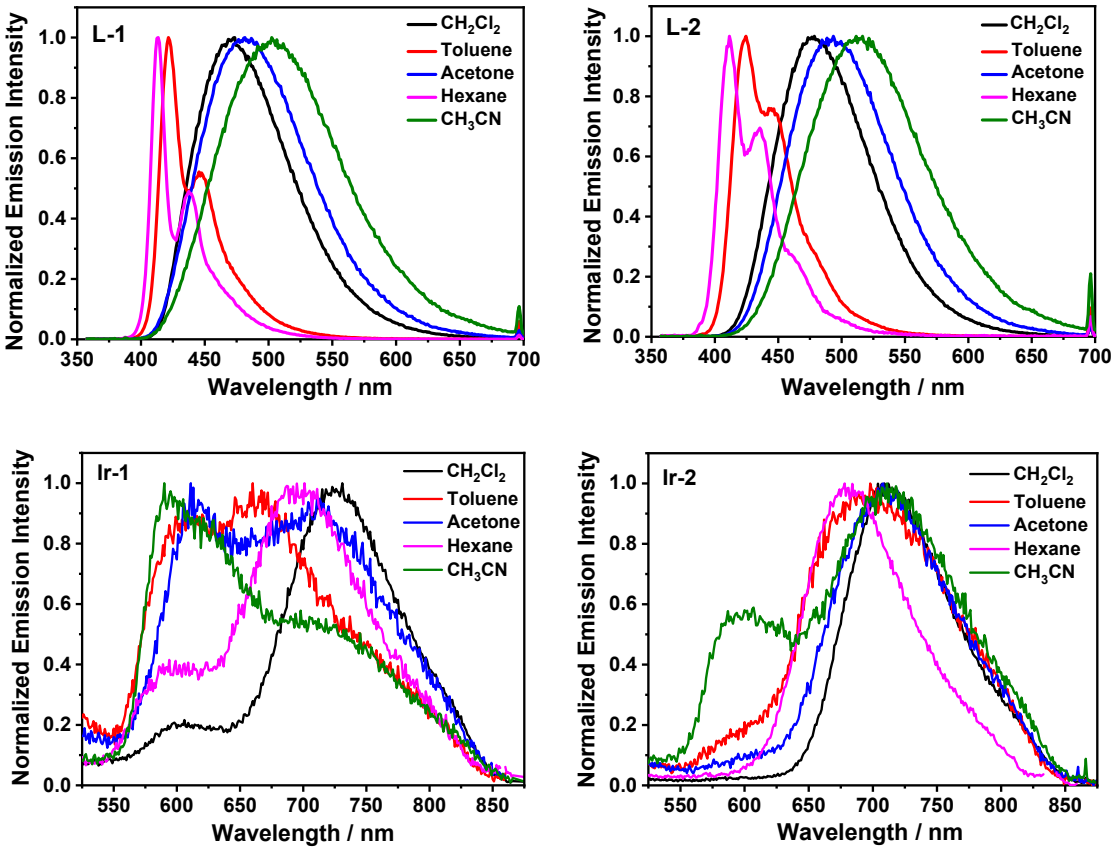

Figure S4. Normalized emission spectra of **L-1**, **L-2**, **Ir-1**, and **Ir-2** in different solvents at room temperature. λ_{ex} = 347.5 nm for **L-1** and **L-2**, and λ_{ex} = 436 nm for **Ir-1** and **Ir-2**.

Table S2. Emission parameters of **L-1**, **L-2**, **Ir-1**, and **Ir-2** in different solvents at room temperature.

	λ_{em}/nm; Φ_{em}[a]				
	Hexane	Toluene	CH_2Cl_2	Acetone	CH_3CN
L-1	413, 438; 0.36	421, 446; 0.52	472; 0.67	481; 0.60	503; 0.43
L-2	412, 435; 0.12	424, 445; 0.52	477; 0.64	493; 0.60	514; 0.41
Ir-1	588, 704; 0.004	610, 668; 0.003	595, 718; 0.004	618, 715; 0.003	590, 618, 700; 0.003
Ir-2	705; 0.006	707; 0.003	710; 0.006	714; 0.003	588, 716; 0.003

[a] Emission band maxima (λ_{em}) and quantum yields (Φ_{em}) measured in different solvents at room temperature with $Ru(bpy)_3Cl_2$ in degassed CH_3CN (Φ_{em} = 0.097, λ_{ex} = 436 nm) as the reference for complexes **Ir-1** and **Ir-2** and a 1 N sulfuric acid solution of quinine bisulfate (Φ_{em} = 0.546, λ_{ex} = 347.5 nm) as the reference for ligands **L-1** and **L-2**.

Table S3. NTOs representing the fluorescence emitting states for **L-1** and **L-2** in CH_2Cl_2.

	S_1	Electron	Hole
L-1	458 nm	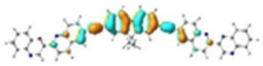	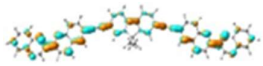
L-2	492 nm		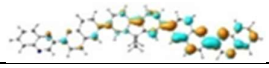

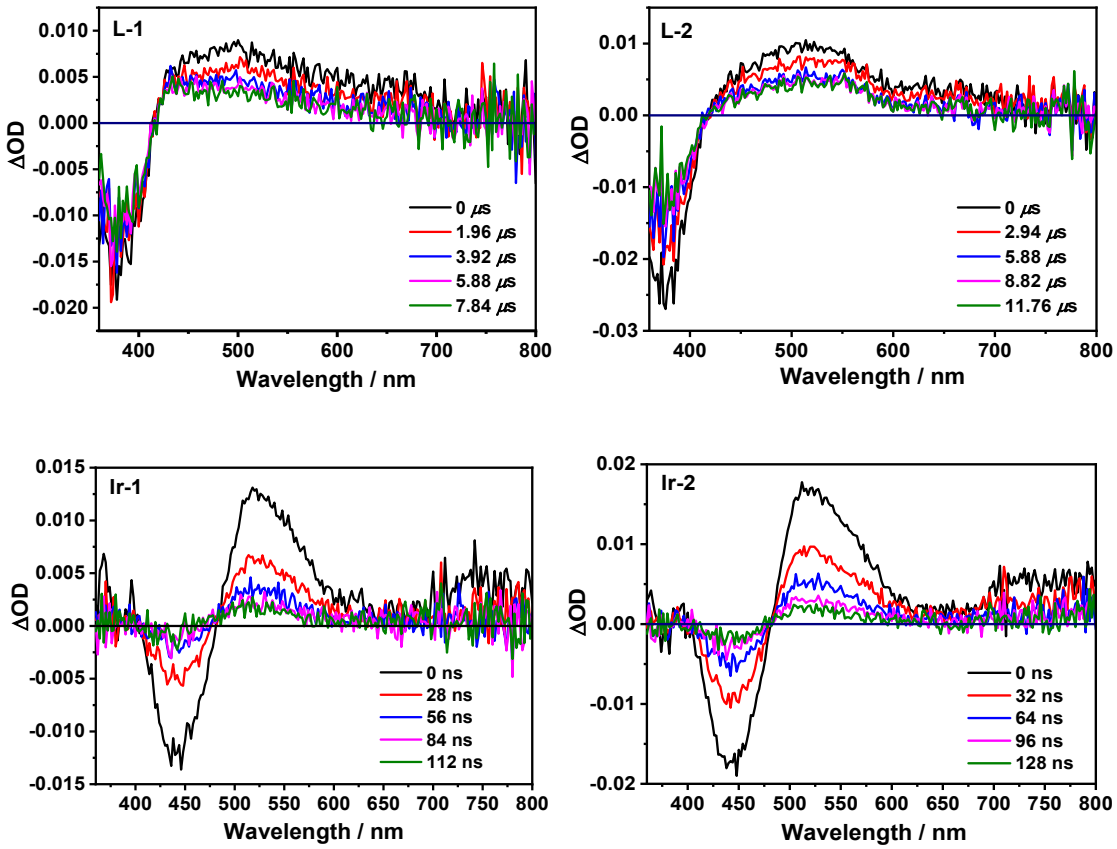

Figure S5. Time-resolved nanosecond TA spectra of **L-1** and **L-2** in CH_2Cl_2, and **Ir-1** and **Ir-2** in CH_3CN after 355-nm excitation. A_{355} = 0.4 in a 1-cm cuvette.